

Article

The Role of Swelling in the Regulation of OPA1-Mediated Mitochondrial Function in the Heart In Vitro

Xavier R. Chapa-Dubocq¹, Keishla M. Rodríguez-Graciani¹, Jorge García-Báez¹, Alyssa Vadovsky², Jason N. Bazil²  and Sabzali Javadov^{1,*} 

¹ Department of Physiology, University of Puerto Rico School of Medicine, San Juan, PR 00936-5067, USA; xavier.chapa@upr.edu (X.R.C.-D.); keishla.rodriguez20@upr.edu (K.M.R.-G.); jorge.garcia25@upr.edu (J.G.-B.)

² Department of Physiology, Michigan State University, East Lansing, MI 48824-1046, USA; vadovsky@msu.edu (A.V.); jnbazil@msu.edu (J.N.B.)

* Correspondence: sabzali.javadov@upr.edu

Abstract: Optic atrophy-1 (OPA1) plays a crucial role in the regulation of mitochondria fusion and participates in maintaining the structural integrity of mitochondrial cristae. Here we elucidate the role of OPA1 cleavage induced by calcium swelling in the presence of Myls22 (an OPA1 GTPase activity inhibitor) and TPEN (an OMA1 inhibitor). The rate of ADP-stimulated respiration was found diminished by both inhibitors, and they did not prevent Ca²⁺-induced mitochondrial respiratory dysfunction, membrane depolarization, or swelling. L-OPA1 cleavage was stimulated at state 3 respiration; therefore, our data suggest that L-OPA1 cleavage produces S-OPA1 to maintain mitochondrial bioenergetics in response to stress.

Keywords: heart mitochondria; OPA1; mitochondrial swelling; membrane potential; calcium retention capacity; mitochondrial respiration



Citation: Chapa-Dubocq, X.R.; Rodríguez-Graciani, K.M.; García-Báez, J.; Vadovsky, A.; Bazil, J.N.; Javadov, S. The Role of Swelling in the Regulation of OPA1-Mediated Mitochondrial Function in the Heart In Vitro. *Cells* **2023**, *12*, 2017. <https://doi.org/10.3390/cells12162017>

Academic Editors: M.-Saadeh Suleiman and Nickolay Brustovetsky

Received: 18 June 2023

Revised: 3 August 2023

Accepted: 4 August 2023

Published: 8 August 2023



Copyright: © 2023 by the authors. Licensee MDPI, Basel, Switzerland. This article is an open access article distributed under the terms and conditions of the Creative Commons Attribution (CC BY) license (<https://creativecommons.org/licenses/by/4.0/>).

1. Introduction

Mitochondria are intracellular organelles which consist of two membranes known as the inner mitochondrial membrane (IMM) and the outer mitochondrial membrane (OMM); these together form the intermembrane space between them as well as the matrix. The IMM is subdivided into two morphologically different domains known as the inner boundary membrane (the IMM regions in proximity to the OMM) and the cristae membrane (the invaginated regions of the IMM). Cristae morphology dictates mitochondrial respiratory capacity, since the cristae are the main IMM regions responsible for energy conversion [1,2]. The cristae membrane contains an abundance of proteins such as the ETC complexes, F₀F₁-ATP synthase, optic atrophy 1 (OPA1) and the mitochondrial contact site and cristae organizing system (MICOS) that regulate mitochondrial function. In response to various physiological stimuli, mitochondria undergo cristae remodeling to maintain their functional stability. Under stress conditions associated with increased reactive oxygen species and Ca²⁺ overload, the MICOS multicomplex and OPA1 can be disrupted, which would impair the structural integrity of the cristae junctions and ultimately result in mitochondrial respiratory defects.

OPA1 is a mitochondrial dynamin-like GTPase which, in addition to the fusion of mitochondria, has been shown to play a key role in the maintenance and stability of the cristae structure [2]. In humans, OPA1 exists as eight different isoforms which can be expressed as combinations of long (L) and short (S) forms known as L-OPA1 and S-OPA1, respectively [3]. The different isoforms of OPA1 can be oligomerized to maintain tight cristae junctions and thereby prevent cytochrome c release from the intercrystal space [4]. In addition, through interaction with cardiolipin, the main phospholipid of the mitochondria, L-OPA1 acts as a contact site to tether with the L-OPA1 of another mitochondrion, thereby

facilitating IMM fusion [5]. Regulating mitochondrial fusion and the formation of cristae junctions is important for mitochondrial quality control and cell viability.

YME1L and OMA1 are the primary enzymes involved in the proteolytic cleavage of L-OPA1. Under physiological conditions, L-OPA1 is cleaved by the ATP-dependent metalloprotease YME1L to form S-OPA1. However, under stress conditions accompanied by membrane depolarization and ATP depletion, YME1L is rapidly degraded, and the ATP-independent zinc metalloprotease OMA1 is activated and becomes the primary enzyme for L-OPA1 cleavage [6]. L-OPA1 is cleaved at different amino acid sequence sites; OMA1 cleaves at the S1 site whereas YME1L cleaves at the S2 site [7]. L-OPA1 has been demonstrated to be the main component in stabilizing the cristae structure in comparison to S-OPA1, which has a less significant stabilizing role [8,9]. Several studies have shown that increased S-OPA1 levels due to L-OPA1 cleavage are associated with altered metabolic activity of mitochondria [10–13]. However, recent genetic studies have found that S-OPA1 can maintain both mitochondrial cristae structure and respiratory activity, even when the mitochondria lack fusion capacity [9,14]. Currently, the role of S-OPA1 in the structural organization of mitochondrial cristae and regulation of mitochondrial function remains unclear.

We have previously shown that Ca^{2+} -induced mitochondrial swelling stimulates proteolytic cleavage of L-OPA1 in isolated cardiac mitochondria [15]. This would suggest that maintaining L-OPA1 integrity may be beneficial under stress conditions such as Ca^{2+} -induced mitochondrial swelling. Myls22, a pharmacological compound, serves as an inhibitor of the GTPase activity exhibited by both L-OPA1 and S-OPA1. By virtue of its inhibitory properties, Myls22 effectively impedes mitochondrial fusion activity. Recent studies have demonstrated that the inhibition of OPA1 GTPase activity by Myls22 is protective against breast cancer growth [16]. Similarly, inhibition of OMA1 by N,N,N',N'-tetrakis-(2-pyridylmethyl)ethylenediamine (TPEN) reduced mitochondrial damage induced by optic nerve injury in C57BL/6J mice [17], suggesting beneficial effects of L-OPA1 under stress conditions. It is important to mention, however, that TPEN's ability to chelate zinc may have unspecific impacts on mitochondria. In this study, we sought to clarify the relationship between L-OPA1 cleavage and the respiratory function of mitochondria using pharmacological inhibitors rather than genetic silencing. We showed that L-OPA1 cleavage was favorable under ADP-stimulated respiration (state 3), suggesting a potential role of S-OPA1 in mitochondrial bioenergetics. This study also demonstrates that inhibition of both OPA1 and OMA1 is ineffective in preventing mitochondrial dysfunction at high Ca^{2+} ; therefore, the role of OPA1 for maintaining IMM structural integrity and function may be limited under pathological conditions.

2. Materials and Methods

2.1. Animals

Male Sprague Dawley rats (275–325 g) were purchased from Taconic (Hillside, NJ, USA). All the experiments were performed according to protocols approved by the UPR Medical Sciences Campus Institutional Animal Care and Use Committee and conformed to the National Research Council Guide for the Care and Use of Laboratory Animals published by the US National Institutes of Health (2011, eighth edition).

2.2. Cardiac Mitochondria Isolation

The isolation of mitochondria was adopted and modified from previous studies [18]. Briefly, both heart ventricles were cut and homogenized using a Polytron homogenizer in 20 mL ice-cold sucrose buffer containing (in mM): 300 sucrose, 20 Tris-HCl, and 2 EGTA, pH 7.2, and supplemented with 0.05% fatty acid-free BSA. The heart homogenate was centrifuged at $2000\times g$ for 3 min to remove cell debris. The supernatant was centrifuged at $10,000\times g$ for 6 min to precipitate the mitochondria in the sucrose buffer (BSA-free) and then washed again under the same conditions in a swelling assay buffer to reduce the EGTA concentration. The final pellet containing the mitochondria was resuspended in 300 μL

of the swelling assay buffer with a final concentration of ~10–15 $\mu\text{g}/\mu\text{L}$. The swelling assay buffer contained (in mM): 125 KCl, 20 MOPS, 10 Tris-HCl, 2 MgCl_2 , 0.001 EGTA, and 2 KH_2PO_4 , pH 7.1.

2.3. Analysis of mPTP Opening

The swelling of the mitochondria in the presence or absence of Ca^{2+} was determined using freshly isolated mitochondria (50 μg) by monitoring the decrease in light scattering at 525 nm as previously described, with minor modifications [18]. The experiments were performed on a CLARIOstar microplate reader (BMG Labtech, Cary, NC, USA) using a 96-well plate. The swelling curves were averaged and presented as their mean absorbance value. The experiments were performed at 37 °C in 0.1 mL of swelling assay buffer or in a hypotonic buffer containing (in mM): 25 KCl, 20 MOPS, 10 Tris-HCl, 2 MgCl_2 , 0.001 EGTA, and 2 KH_2PO_4 , pH 7.1. The pore-forming agent alamethicin was used to induce complete mitochondrial swelling [19].

2.4. Calcium Retention Capacity (CRC) Assay

The CRC was measured by the Ca^{2+} -sensitive fluorescence dye Fluo-5N which reacts to extramitochondrial Ca^{2+} in the assay buffer [20]. Briefly, freshly isolated mitochondria (50 μg or 0.5 mg/mL) were incubated at 37 °C in 0.1 mL of swelling assay buffer containing 500 nM of Fluo-5N. Exogenous Ca^{2+} was added to increase the matrix Ca^{2+} load, and the fluorescence intensity was recorded by means of a CLARIOstar microplate reader (BMG Labtech, Cary NC, USA) using a 96-well plate. The CRC curves were averaged and presented as fluorescence intensity (relative fluorescent units).

2.5. Analysis of Mitochondrial Respiration and Membrane Potential

Measurement of mitochondrial respiration and membrane potential was performed at 37 °C using an Oxygraph 2k (Oroboros Instruments Corp., Innsbruck, Austria). The O2k chambers were loaded with 2 mL of a swelling assay buffer that contained (in mM): 125 KCl, 20 MOPS, 10 Tris-HCl, 2 MgCl_2 , 0.001 EGTA, and 2 KH_2PO_4 , pH 7.1. All the subsequent experiments were performed using this buffer and temperature. At 0 min, the inhibitors (as indicated in figures) 2.5 mM 2-oxoglutarate and 1 mM L-malate (OM) as well as 0.1 μM of the lipophilic cationic dye TMRM were added, followed by 0.1 mg/mL of mitochondria. Here, we considered state 2 respiration as the rate of oxygen consumption by the mitochondria only in the presence of substrates, whereas state 3 was performed in the presence of 1 mM ADP in addition to the substrates. At 5 min, a 600 nmol/mL bolus of Ca^{2+} was added to induce mitochondrial swelling. At 10 min, a 1 mM bolus of ADP was added to induce maximal ADP-stimulated (state 3) respiration. An alternative experiment was performed in which we assessed the same parameters with ADP added at 0 min and the Ca^{2+} bolus at 5 min. The ratiometric approach (546/573 nm excitation, 590 nm emission) was applied to calculate the membrane potential on the basis of the TMRM fluorescence activity by the following equation: $\frac{F(t=0)-F(t)}{F_{\text{max}}-F_{\text{min}}}$ [21]. This equation is utilized to evaluate changes in fluorescence intensity and allows for the normalization of the fluorescence signal. Several factors, such as fluorescent molecule concentration, excitation intensity, and instrument variations, can influence fluorescence intensity. However, the equation enables researchers to determine the relative change in fluorescence intensity independent of these factors, thereby providing a direct correlation to the biological process under scrutiny.

2.6. SDS-PAGE and Western Blotting

Equal numbers of mitochondrial proteins were resolved by SDS-PAGE and transferred overnight to nitrocellulose membranes (GE Healthcare Bio-Sciences, Piscataway, NJ, USA). Then the membranes were immunoblotted with OPA1 (#612607, BD Biosciences, Franklin Lakes, NJ, USA,) and ATP5A (#ab14748, Abcam, Boston, MA, USA,). Images were acquired using the Odyssey CLx Infrared Imaging System (LI-COR Biosciences, Lincoln, NE, USA).

Image analysis was performed using ImageJ (version 1.52a) software from NIH. The L-OPA1, and S-OPA1 levels were quantified as a percentage of the total OPA1.

2.7. Statistical Analysis

The data values for the bar graphs are presented as mean \pm SE, whereas time series plots are presented by only the mean. The number of biological samples, but not technical replicates, were used as a sample size. The data were analyzed using the one-way ANOVA and Student's t-tests for the comparison of independent groups via a GraphPad prism (version 9).

3. Results

3.1. The Effects of Myls22 and TPEN on Mitochondrial CRC

In the first set of experiments, we evaluated the effects of Myls22 and TPEN on the CRC of isolated heart mitochondria. Considering that L-OPA1, but not S-OPA1, is the main component in stabilizing the cristae structure, we proposed that inhibition of L-OPA1 cleavage through blocking OMA1 activity by TPEN could maintain the IMM structural integrity, increase its resistance to swelling, and enhance the CRC of the mitochondria in response to Ca^{2+} . S-OPA1 generated by L-OPA1 cleavage has been shown to retain the GTPase activity and contain all of the functional domains of OPA1 [22]. It should be noted that the zinc-chelating capacity of TPEN may have nonspecific effects on mitochondria. On the other hand, Myls22 can inhibit the GTPase activity of both L-OPA1 and S-OPA1, which is used to prevent fusion activity, thereby limiting the OPA1 function to maintaining the cristae structure [16]. Mitochondria suspensions (50 μg per well) were incubated with Myls22 and TPEN at a range of 12.5–100 μM and 1.25–10 μM , respectively, in the presence of complex I substrates alone (OM group) or in combination with ADP (OM+ADP group). ADP was added to assess the contribution of mitochondrial permeability pores (mPTP)-independent and mPTP-dependent swelling. The concentration ranges for Myls22 and TPEN were based on previous studies [23,24]. The results showed that in the presence of OM, Myls22 was effective at all concentrations (Figure 1A), whereas TPEN was most effective at 2.5–10 μM (Figure 1B) to increase the CRC of the mitochondria by reducing the rate of Ca^{2+} release. The effects of Myls22 and TPEN on the CRC were negligible in comparison to 1 μM sangliferrin A (SfA, a mPTP inhibitor, positive control). In the presence of OM and ADP, Myls22 and TPEN at all concentration ranges had no noticeable effect on the CRC (Figure 1C,D). Based on concentration-dependent data, 50 μM Myls22 and 5 μM TPEN were used in the next sets of experiments.

3.2. The Effects of Myls22 and TPEN on Mitochondrial Function

In these experiments, we examined the effects of Myls22 and TPEN on mitochondria by assessing mitochondrial swelling, respiration, and membrane potential. We found that Myls22 and TPEN did not have any negative effects on mitochondrial swelling in the presence of OM (OM group) or OM and ADP (OM+ADP group) (Figure 2A,B). Likewise, mitochondrial respiration rates (state 2 and state 3) (Figure 2C,D) and membrane potential (Figure 2E,F) were not affected by Myls22 and TPEN; however, they were significantly reduced by alamethicin and hypotonic conditions.

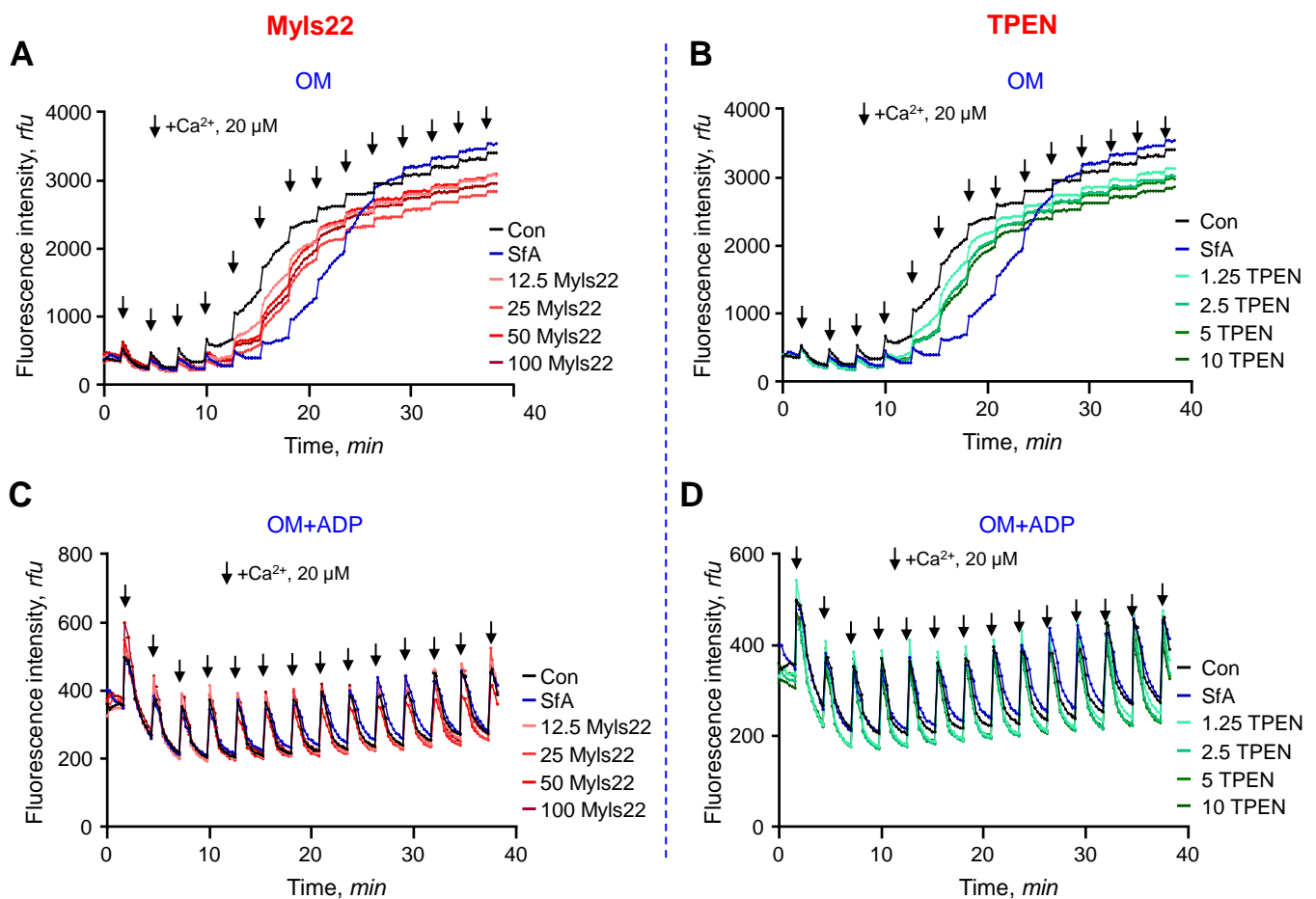


Figure 1. Dose-dependent effects of Myls22 and TPEN on the CRC of isolated cardiac mitochondria. Dose-dependent experiments were conducted using Myls22 (OPA1 inhibitor) and TPEN (OMA1 inhibitor) to determine the effective concentration of each inhibitor. The CRC of mitochondria (0.5 mg/mL) was analyzed in the presence of OM alone (OM group) or in combination with ADP (OM+ADP group). Ca^{2+} was added every 3 min, indicated by arrows, with an incremental increase of 20 μM per pulse. (A,B) OM group, (C,D) OM+ADP group. Concentration ranges for Myls22 (A,C) and TPEN (B,D) were 12.5–100 μM and 1.25–10 μM , respectively. $n = 3$ per group.

Next, we evaluated the effects of Myls22 and TPEN on mitochondria exposed to Ca^{2+} -induced swelling in the presence of OM (Figure 3) or OM and ADP (Figure 4). We found that Myls22, TPEN, and SfA were not able to prevent the Ca^{2+} -induced inhibition of mitochondrial respiration and dissipation of the membrane potential in the presence of OM (no ADP) (Figure 3A–D). Likewise, Myls22 and TPEN had no effects whereas SfA reduced Ca^{2+} -induced swelling and increased the CRC of the mitochondria (Figure 3E,F). Interestingly, Myls22 and TPEN significantly reduced mitochondrial respiration (~72% and ~74%) in the presence of OM and ADP (state 3) upon Ca^{2+} addition in comparison to the control group (no Ca^{2+}) (Figure 4A,B). However, the mitochondrial membrane potential was sustained after the addition of Ca^{2+} (Figure 4C,D), demonstrating the protective effects of ADP. In the presence of OM and ADP, Ca^{2+} -induced mitochondrial swelling was not affected by Myls22. However, both TPEN and SfA (reduced by ~30% and 78%, respectively) had a protective effect and attenuated Ca^{2+} -induced mitochondrial swelling (Figure 4E,F). Similarly, both Myls22 and TPEN demonstrated no effects on the mitochondrial CRC, indicating the absence of an mPTP opening under this condition (Figure 4G). Additionally, we performed the same experiments with low Ca^{2+} (300 nmol/mL Ca^{2+}) while evaluating mitochondrial respiration and membrane potential. Like high Ca^{2+} concentration, Myls22 and TPEN had no protective effects on mitochondrial respiration and membrane potential

at low Ca^{2+} (Figure S1A–D). The results of these experiments demonstrate that TPEN and SfA, but not Myls22, prevent mPTP-independent mitochondrial swelling under high Ca^{2+} conditions with no protective effects on mitochondrial function.

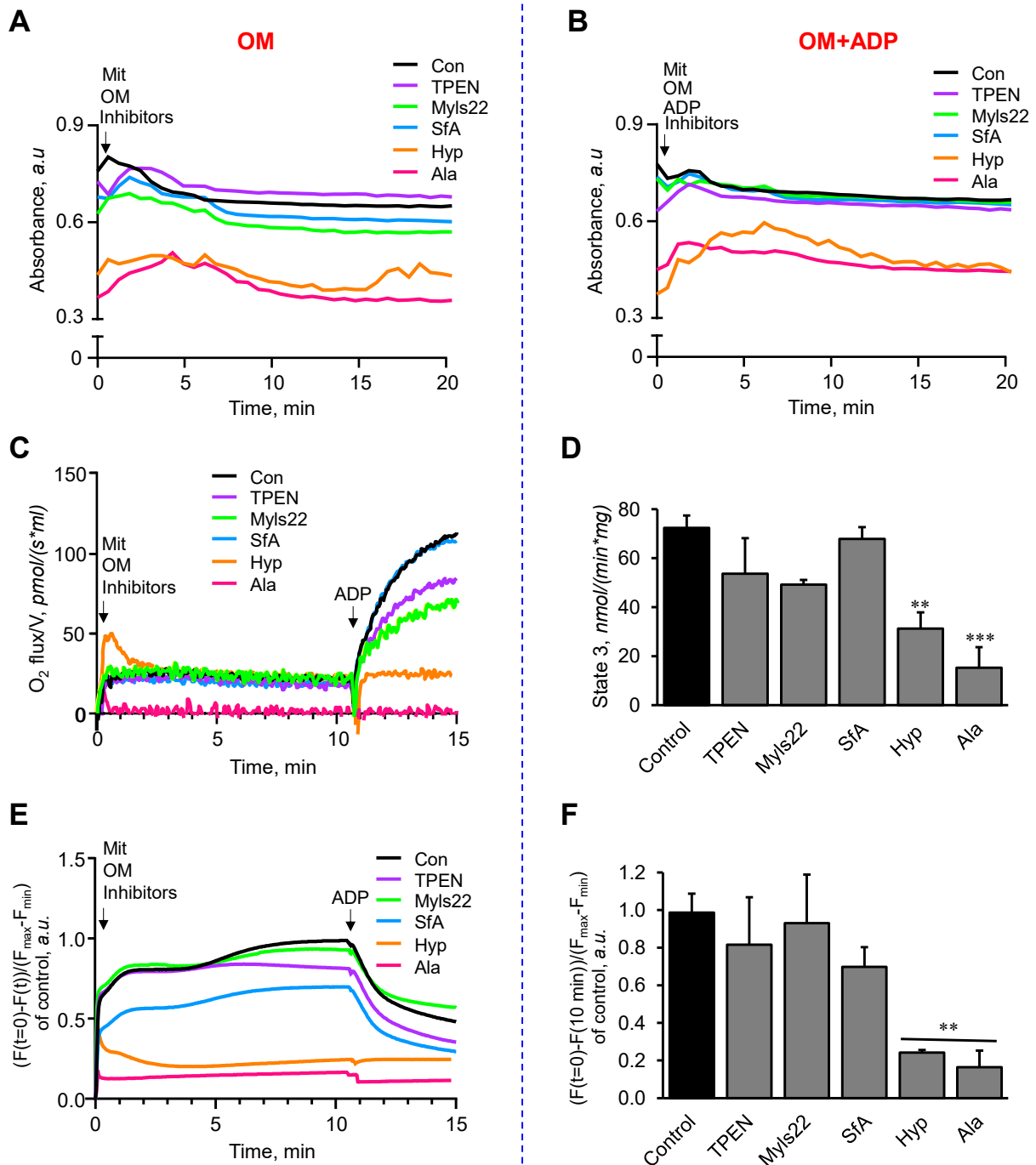


Figure 2. The effects of Myls22 and TPEN on mitochondrial swelling, membrane potential, and respiration. Mitochondrial swelling (A,B), mitochondrial respiration (C,D), and membrane potential (E,F) were analyzed in the presence and absence of ADP. Mitochondrial swelling was measured by TMRM separately in the OM (A) and OM+ADP (B) groups, whereas mitochondrial respiration (C,D) and membrane potential (E,F) were determined simultaneously by adding ADP following basal conditions. All three parameters were measured in the presence of Myls22 (50 μ M), TPEN (5 μ M), SfA (0.5 μ M), hypotonic medium (Hyp), and alamethicin (Ala, 10 μ M). $n = 3$ per group. ** $p < 0.01$ and *** $p < 0.001$ vs. Con.

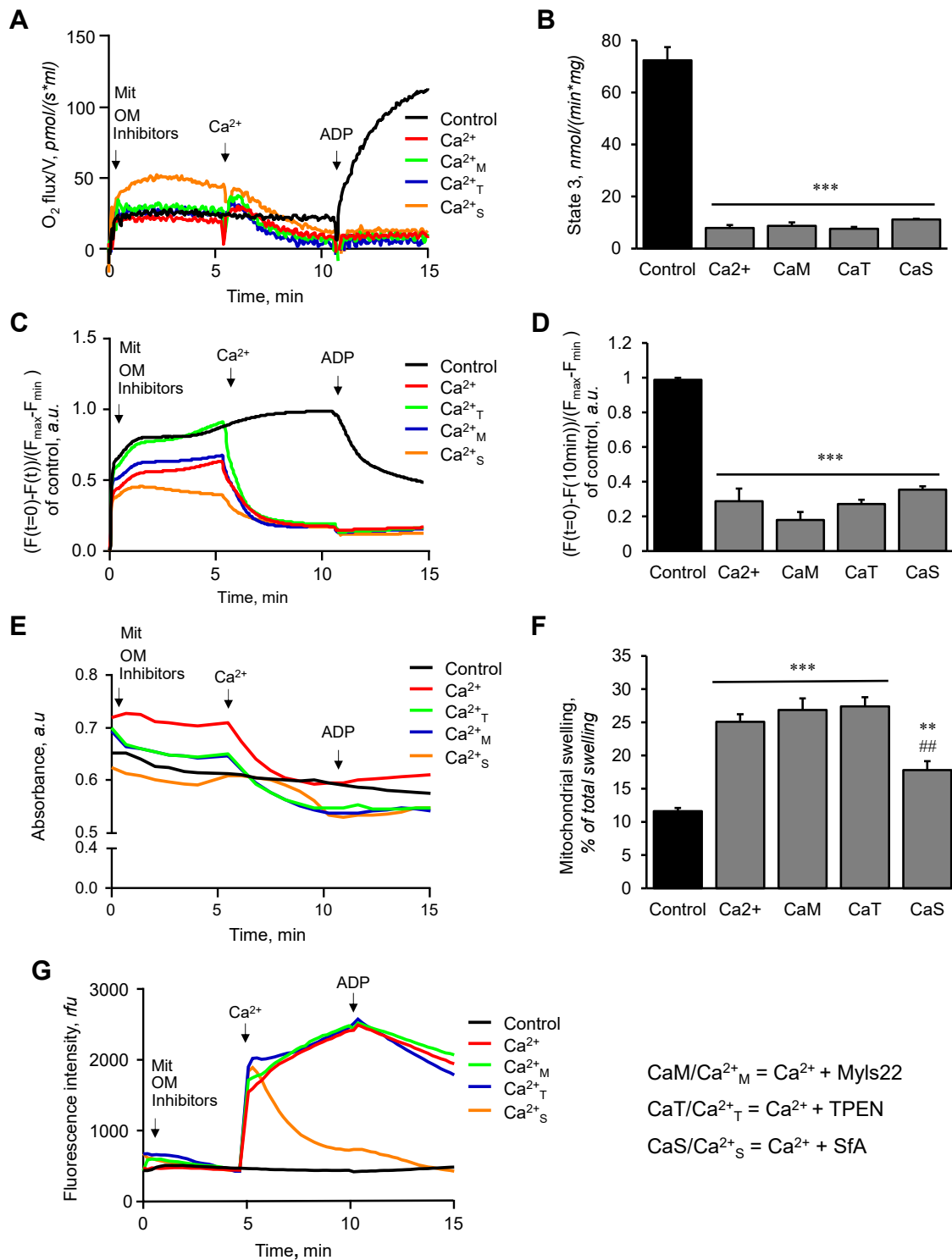


Figure 3. The effects of Myls22 and TPEN on the functional state of mitochondria in the presence of Ca^{2+} . The effects of Myls22 and TPEN on mitochondrial respiration (A,B), membrane potential (C,D), swelling (E,F), and CRC (G) were analyzed in the presence of Ca^{2+} (600 nmol/mL) and respiration substrates (OM). Quantitative data are presented for state 3 respiration rate (B) at 15 min and for membrane potential (D) and mitochondrial swelling (F) at 10 min after addition of Ca^{2+} and ADP. The inhibitors OM and TMRM (0.1 μM) were added 5 min prior to the addition of the mitochondria. Ca^{2+} and ADP (1 mM) were added, respectively, 5 min and 10 min after the addition of the mitochondria. All experiments were terminated at 15 min. $n = 3$ per group. $** p < 0.01$ and $*** p < 0.001$ vs. Con; $## p < 0.01$ vs. Ca^{2+} .

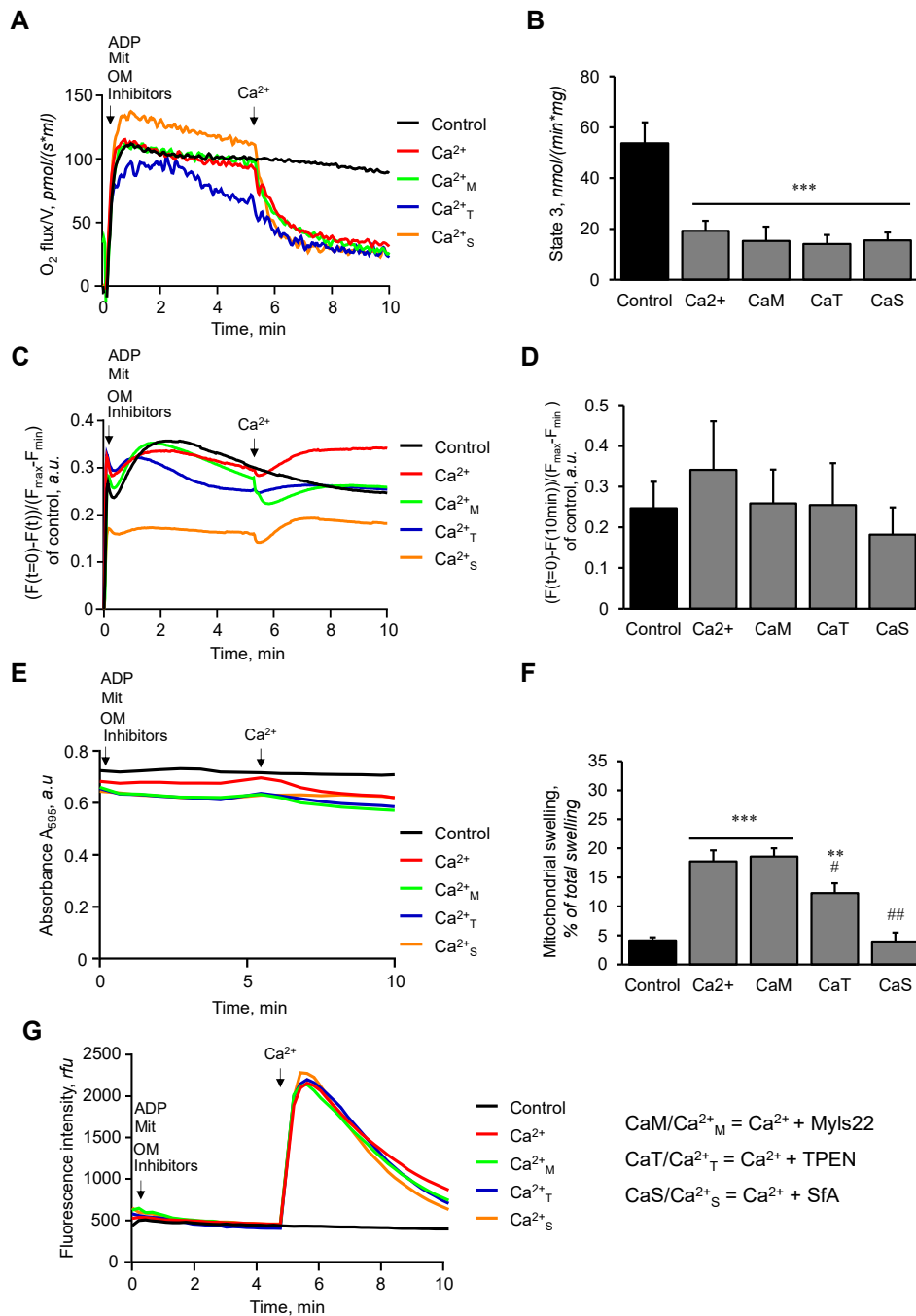


Figure 4. The effects of Myls22 and TPEN on the functional state of mitochondria in the presence of ADP. The effects of Myls22 and TPEN on mitochondrial respiration (A,B), membrane potential (C,D), swelling (E,F), and CRC (G) were analyzed in the presence of Ca²⁺ (600 nmol/ml), OM, and ADP. Quantitative data for state 3 respiration rate (B), membrane potential (D), and mitochondrial swelling (F) are presented at 10 min after addition of Ca²⁺. The inhibitors OM, ADP, and TMRM were added 5 min prior to the addition of the mitochondria, and Ca²⁺ was added 5 min after the addition of the mitochondria. All experiments were terminated at 10 min. n = 3 per group. ** p < 0.01 and *** p < 0.001 vs. Con; # p < 0.05 and ## p < 0.01 vs. Ca²⁺.

3.3. L-OPA1 Cleavage under Distinct Mitochondrial Energetic and Swelling Conditions

Next, we evaluated L-OPA1 cleavage by analysis of L-OPA1 and S-OPA1 protein levels in the samples from the experiments described in 3.2. We found that mitochondria treated with Ca²⁺ or alamethicin (reduced ~58% and ~86%) in the presence of OM alone

(OM group) contained low L-OPA1 levels (Figure 5A). In the presence of OM and ADP (OM+ADP group), Ca²⁺ had no effects, whereas alamethicin or hypotonic medium reduced (approximately 30% and 31%, respectively) L-OPA1 levels (Figure 5B). A hypotonic medium was used to clarify whether an increase in mitochondrial volume can affect the integrity of L-OPA1. As expected, Myls22 and TPEN, but not SfA, attenuated Ca²⁺-induced cleavage of L-OPA1 in the presence of OM as evidenced by high levels of L-OPA1 (approximately 64% and 72% for Myls22 and TPEN, respectively) and low levels of S-OPA1 in these groups compared to the Ca²⁺-treated group used as a control (untreated with Myls22 and TPEN) (Figure 5C). Interestingly, Myls22, TPEN, and SfA had no effects on L-OPA1 levels in mitochondria treated with OM and ADP (OM+ADP group) in the presence of Ca²⁺ (Figure 5D). Next, we compared the protein levels of L-OPA1 and S-OPA1 in the presence of either hypotonic medium or the swelling assay buffer (Figure 6A,B). The results showed that the mitochondria contained less L-OPA1 and high S-OPA1 levels in both the hypotonic medium and the swelling assay buffer in the presence of OM and ADP (OM+ADP group) compared to the OM group. Altogether, these data demonstrate that cleavage of L-OPA1 is stimulated at state 3 respiration but not at state 2, suggesting that L-OPA1 cleavage requires high OXPHOS activity.

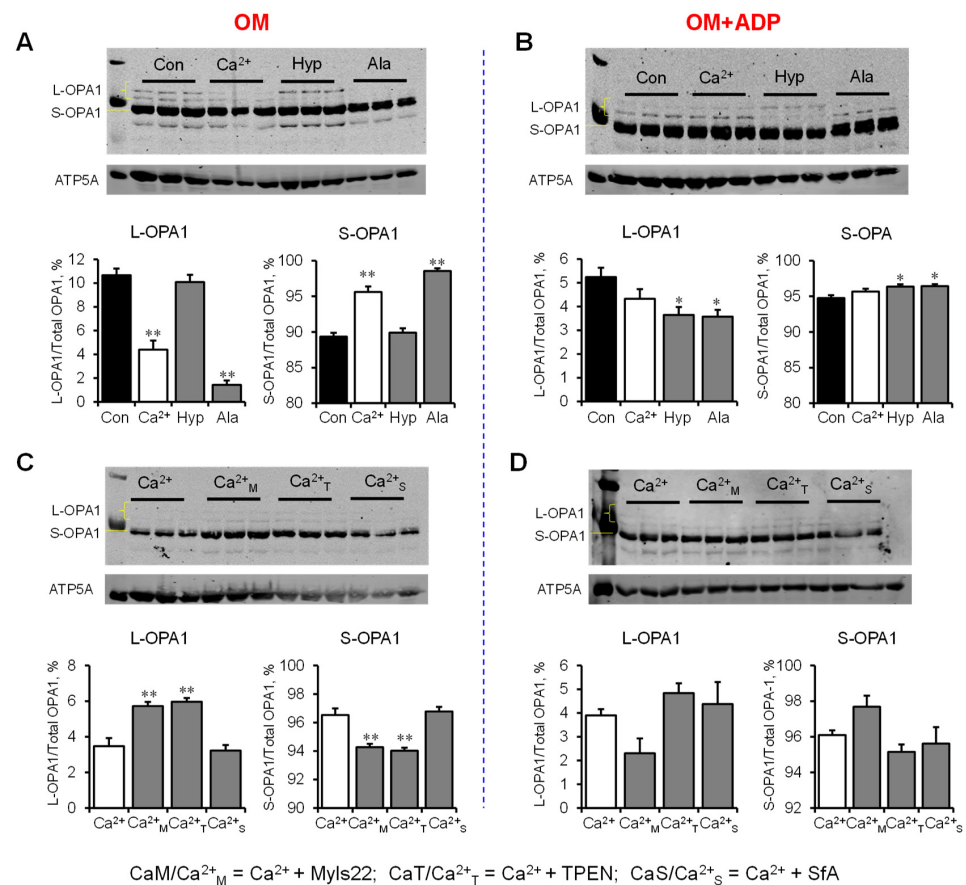


Figure 5. The effects of Myls22 and TPEN on L-OPA1 cleavage under different swelling conditions in mitochondria. L-OPA1 and S-OPA1 protein levels in OM (A,C) and OM+ADP (B,D) groups. L-OPA1 cleavage was induced by distinct swelling inducers, including Ca²⁺ (600 nmol/ml), alamethicin (Ala, 10 μM), and hypotonic solution (Hyp) in the presence and absence of Myls22, TPEN, and SfA. L-OPA1 and S-OPA1 were separated using SDS-PAGE and identified by Western blotting using specific OPA1 antibodies. The data obtained from the blots were analyzed using ImageJ software, and the protein levels of L-OPA1 and S-OPA1 were normalized to total OPA1 and expressed as a percentage. ATP5a was used as a loading control. n = 3 per group. * p < 0.05, ** p < 0.01 vs. Control (Con) for (A,B) or vs. Ca²⁺ for (C,D).

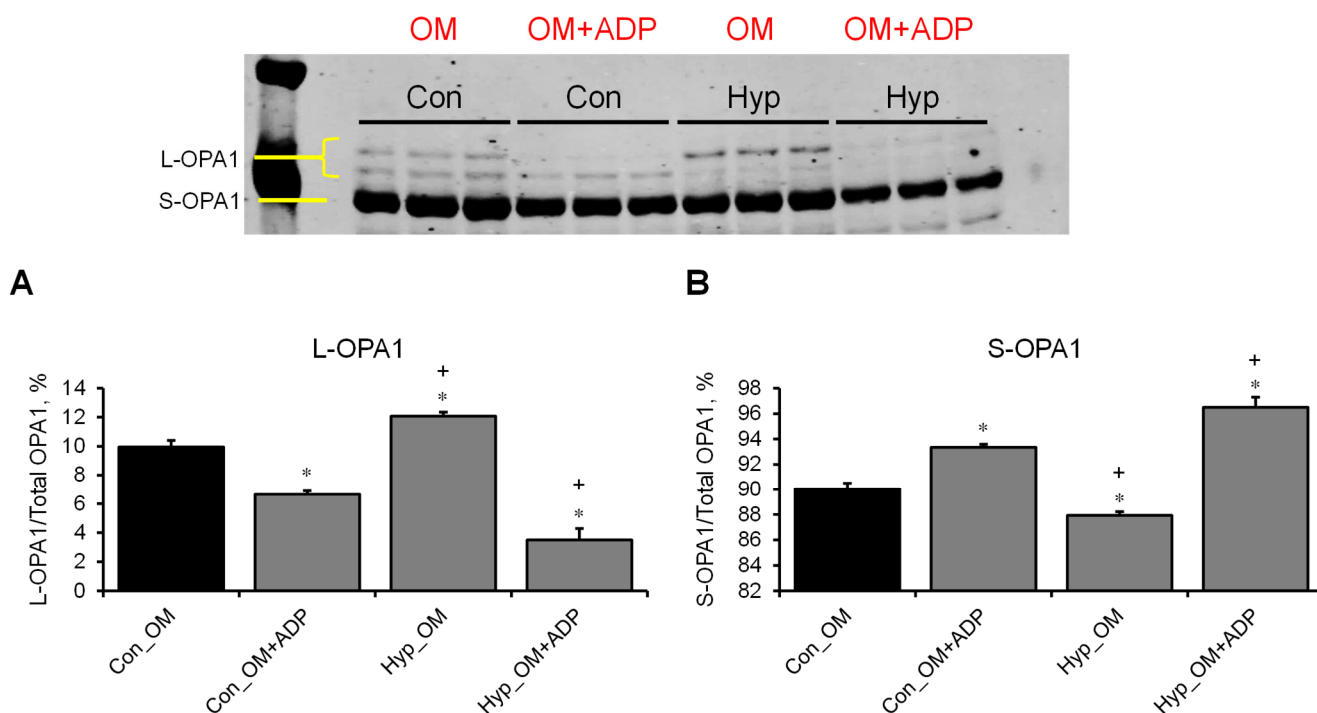


Figure 6. The effects of ADP on L-OPA1 cleavage under hypotonic conditions. The protein levels of L-OPA1 (A) and S-OPA1 (B) were assessed in OM and OM+ADP groups in isotonic (Con) and hypotonic (Hyp) conditions. L-OPA1 and S-OPA1 were separated using SDS-PAGE and identified by Western blotting using specific OPA1 antibodies. The data obtained from the blots were analyzed using ImageJ software, and the protein levels of L-OPA1 and S-OPA1 were normalized to total OPA1 and expressed as a percentage. $n = 3$ per group. * $p < 0.01$ vs. Con_OM and $^+ p < 0.01$ vs. Con_OM+ADP.

4. Discussion

Although the role of OPA1 in mitochondrial swelling has been thoroughly investigated, few studies have elaborated on the relationship between OPA1 cleavage and mitochondrial swelling. This study, for the first time, demonstrates a relationship between mitochondrial respiration and L-OPA1 cleavage under physiological conditions. We showed that an increase in mitochondrial respiration leads to more L-OPA1 cleavage, whereas a lower respiratory state is associated with less L-OPA1 cleavage. Next, we demonstrated that Myls22 and TPEN are ineffective in preventing mitochondrial swelling in OM groups even though both agents are effective in partially preventing L-OPA1 cleavage. Moreover, Myls22 and TPEN did not affect the functional state of mitochondria and OPA1 cleavage in the presence of OM and ADP, even though TPEN had some protective effect against mitochondrial swelling. These data suggest that, in addition to its role in fusion, L-OPA1, as well as S-OPA1, can participate in the regulation of the respiratory function of mitochondria.

Using Myls22 and TPEN, we demonstrated that the normal functioning of mitochondria (membrane potential and respiration) requires the structural integrity of the total OPA1 (both L- and S-OPA1). It should be noted that control (untreated) mitochondria isolated from healthy hearts contain a large proportion of S-OPA1, which accounts for ~90% of the total OPA1 (under these experimental conditions). This suggests that S-OPA1 can play a structural and/or functional role in mitochondria. In the present study, a K^+ -based medium was used to replicate cytosolic conditions at 37 °C for 15 min, which better represents a natural setting for evaluating mitochondrial swelling. However, it is important to note that K^+ induces a background swelling process [25] due to the influx of K^+ when the mitochondria replenish the lost K^+ during the isolation procedure. In previous studies, we employed a sucrose-based swelling buffer that lacks basal swelling due to the absence of K^+ , which

typically displays an L-OPA1 isoform percentage in the range of 20–25% [15,26,27]. Considering that changes in mitochondrial volume can impact OPA1 processing, we propose that the K^+ -induced swelling could contribute to the observed discrepancy in the OPA1 expression levels.

We investigated the impact of severe stress conditions and distinct respiratory conditions on the reduction in L-OPA1, a protein essential for mitochondrial activity. As shown in Figure 5, under severe stress conditions (Ca^{2+} stress, alamethicin, hypotonic medium) and distinct respiratory conditions (OM, OM+ADP), we observed only a small reduction in L-OPA1. Interestingly, OPA1 GTPase activity is required for mitochondrial activity; nucleoside diphosphate kinase-D (NDPK-D) converts GDP to GTP by utilizing ATP transported through adenine nucleotide translocase (ANT), which can also play a role in modulating mitochondrial swelling [28,29]. Depletion of total OPA1 has shown the development of mitochondrial dysfunction characterized by respiratory defects, lower membrane potential, and IMM swelling [30,31]. Initially, the generation of S-OPA1 due to L-OPA1 cleavage was considered detrimental and with the potential to lead to cell death [8]. Notably, studies with artificial liposomes demonstrated that S-OPA1 resulting from L-OPA1 cleavage retains GTPase activity and dynamin protein functionality [22], suggesting that S-OPA1 can function as a structural IMM protein and interact with different IMM proteins due to its solubility. In favor of this conclusion, recent studies with expression of exclusively L-OPA1 or S-OPA1 in cells showed that S-OPA1 in the absence of L-OPA1 was able to maintain the cristae structure and activity of mitochondrial bioenergetics [3,9]. This suggests that if OPA1 is present in either short or long isoform, the mitochondria can maintain their functional and structural integrity. Using pharmacological inhibitors, we revealed that the transition of mitochondrial respiration from state 2 to state 3 stimulates OPA1 cleavage. Consistent with our data, experiments measuring mitochondrial respiration in tissues overexpressing OPA1 have demonstrated increased mitochondrial complex I respiration compared to the control samples [2]. This observation suggests that the elevated expression of OPA1 can result in the generation of higher levels of S-OPA1 during states of enhanced respiration. Interestingly, there was no difference in complex I mtDNA levels or translation [2]. Moreover, in mice that were exposed to feeding and starvation states, OPA1 could rapidly and reversibly oligomerize in response to changes in energetic demand due to an interaction between the OPA1 and solute carrier 25A (SLC25A) family proteins [32]. However, that study did not evaluate OPA1 cleavage; therefore, new studies are necessary to clarify the potential role of S-OPA1 in OPA1-SLC25A interaction as well as in OPA1 oligomerization that can be affected by shifts in energy demand.

Mitochondrial OPA1 processing occurs through the enzymatic activity of YME1L and OMA1. Under cellular stress, OMA1 activation is demonstrated to cleave L-OPA1 isoforms and lead to mitochondrial fragmentation, which is an underlying factor for the pathogenesis of many diseases such as cardiac ischemia-reperfusion injury [26,33]. However, the ATP-dependent OPA1 protease YME1L cleaves OPA1 without affecting morphology. Genetic studies evaluating OMA1 and YME1L knockout in mouse embryonic fibroblasts (MEFs) showed that mitochondria in the absence of YME1L become fragmented and cannot sustain mitochondrial cristae structure, whereas the depletion of OMA1 does not exhibit these changes [34]. Additionally, YME1L-deficient spinal cord mitochondria exhibit a late onset of respiratory dysfunction [35], and yet another study showed that OMA1-deficient mouse liver mitochondria did not exhibit respiratory dysfunction under a control diet [36]. Overall, these studies suggest that the distinct OPA1 cleavage sites (the S1 and S2 sites) may play different roles toward mitochondrial function, and therefore YME1L and/or OMA1 may have alternative roles independent of the OPA1 processing.

Myls22, a specific inhibitor of OPA1 GTPase activity, has also been shown to suppress mitochondrial fusion [23,37]. Contrary to our expectations, the results of our study did not demonstrate any modulation of Ca^{2+} -induced mitochondrial swelling by Myls22. Likewise, TPEN, a zinc-chelator and OMA1 inhibitor [17,38], was not effective in preventing Ca^{2+} -induced mitochondrial swelling. It is tempting to speculate that OPA1 oligomerization can

be more essential for maintaining the mitochondrial cristae structure than OPA1 cleavage as demonstrated by the genetically modified MEFs, which were able to maintain a moderate cristae structure with only S-OPA1 expression [9]. Moreover, mice starvation experiments have demonstrated that OPA1 oligomerization is necessary to maintain mitochondrial structural integrity under starvation stress [32]. Additionally, OPA1 oligomerization is targeted during BID activation via apoptosis, thereby aiding in the release of cytochrome c and debilitating the structural integrity of the mitochondrial cristae structure [4,39]. The role of OPA1 oligomerization and its relationship to mitochondrial cristae structure and respiration remain to be elucidated in future studies.

Mitochondrial fusion and fission play a central role in maintaining mitochondrial health during physiological conditions [40–42]. The interplay between mitochondrial dynamics, mitophagy, and biogenesis is important for maintaining mitochondrial quality control. Changes in the structural remodeling of the IMM play a key role in the adaptation of mitochondria to metabolic/energy demands. The balance between mitochondrial dynamics and energy demand is important for the regulation of mitochondrial bioenergetics [43,44]. In favor of this conclusion, ATP depletion induced by 2-deoxyglucose significantly upregulated fusion proteins (Mfn1 and Mfn2) and reduced the fusion protein Drp1 levels in DLD-1 cells [45]. Similar results were obtained in experiments with oxygen-glucose deprivation [46]. The adult rat heart contains all the fission (Drp1, Fis1) and fusion (Mfn1/2, OPA1) proteins [47]. OPA1 is vital in mediating IMM fusion since it works together with cardiolipin to tether distinct membranes for the fusion process [48]. Furthermore, L-OPA1 and S-OPA1 work together to expedite the membrane tethering process; ideally, a 1:1 ratio of [S-OPA1]/[L-OPA1] provides the most effective fusion conditions for mitochondrial membranes [5]. In turn, studies in MEFs involving non-simultaneous knockout of YME1L and OMA1 as well as double knockout revealed that OPA1 processing is not essential for mitochondrial fusion; however, it may play a stimulatory role in mitochondrial fission [34]. These studies suggest that other factors or mechanisms may be involved in regulating mitochondrial fusion independently of OPA1 processing. Subsequently, many studies have focused on the relationship between mitochondrial fusion and fission toward metabolism [49,50]. However, only a few studies have elucidated the mechanism by which mitochondrial respiration can mediate changes in fusion and fission dynamics. OPA1 cleavage by YME1L, not OMA1, has been shown to result in an OXPHOS-stimulated mitochondrial fusion [51]. Our study demonstrates that alterations in the mitochondrial energetic state led to changes in the S-OPA1/L-OPA1 ratio that may play a causal role in membrane fusion events. Further studies are necessary to clarify the molecular mechanisms underlying the effects of distinct metabolic states on mitochondrial dynamics through OPA1 processing.

5. Conclusions

This study provides evidence that L-OPA1 cleavage is associated with mitochondrial respiration, implying that under physiological conditions, L-OPA1 cleavage may favor mitochondrial respiration. Pharmacological inhibition of OPA1 or OMA1 does not affect Ca^{2+} -induced mitochondrial swelling, suggesting that the maintenance of cristae structural integrity by OPA1 occurs through an alternate mechanism(s). OPA1 oligomerization seems to play an important role in maintaining mitochondrial structural and functional integrity during stress conditions.

Limitations

This section aims to acknowledge the limitations of our study and provide a balanced perspective on the findings. Firstly, accurately quantifying faint L-OPA1 bands compared to stronger S-OPA1 bands was challenging and may have introduced uncertainties into the findings. Specifically, as part of our research, we conducted a comparative analysis of the effects of various compounds/factors on L-OPA1 and S-OPA1 under two distinct conditions: (i) preservation of mitochondria in a sucrose buffer on ice and (ii) exposure to a K^{+} -based

swelling assay buffer at 37 °C. We observed an ~15% reduction in L-OPA1 isoforms in the K⁺-based buffer, which caused the L-OPA1 bands to become fainter. Presently, our investigation aims to elucidate the underlying reasons for this observed phenomenon, with particular emphasis on discerning the potential role of passive K⁺-dependent swelling as a plausible contributing factor. Secondly, the focus on measuring changes in mitochondrial volume using the mitochondrial swelling assay might not fully capture all the factors affecting mitochondrial behavior. Complementing this approach with other assays that assess mitochondrial function or morphology could provide a more comprehensive view of mitochondrial dynamics. The absence of Na⁺ in the assay was intended to prevent confounding effects, but it may also limit the generalizability of the results. Another limitation lies in the changes made to the experimental environment, such as using a K⁺-based buffer and incubation at 37 °C, which might alter the OPA1 values. These environmental modifications may introduce variations into the experimental conditions, influencing the behavior of the OPA1 and potentially affecting the accuracy and comparability of the results. Despite these limitations, the study provides valuable insights into mitochondrial dynamics and mPTP regulation, and future research could address these issues to further enhance understanding.

Supplementary Materials: The following supporting information can be downloaded at: <https://www.mdpi.com/article/10.3390/cells12162017/s1>.

Author Contributions: S.J. and J.N.B. conceived and designed the study. X.R.C.-D., J.G.-B., K.M.R.-G., A.V. and J.N.B. performed the experiments and interpreted the results. X.R.C.-D. and S.J. wrote the first draft of the manuscript, and all the authors commented on the manuscript. S.J. supervised the project and is responsible for its integrity. All authors have read and agreed to the published version of the manuscript.

Funding: This study was supported by grants from the National Science Foundation (2006477 to S.J.) and the National Institutes of Health (SC1GM128210 to S.J.).

Informed Consent Statement: Not applicable.

Data Availability Statement: The data that support the findings of this study are available from the corresponding author, upon reasonable request.

Conflicts of Interest: The authors declare no conflict of interest.

References

1. Kuhlbrandt, W. Structure and function of mitochondrial membrane protein complexes. *BMC Biol.* **2015**, *13*, 89. [[CrossRef](#)] [[PubMed](#)]
2. Cogliati, S.; Frezza, C.; Soriano, M.E.; Varanita, T.; Quintana-Cabrera, R.; Corrado, M.; Cipolat, S.; Costa, V.; Casarin, A.; Gomes, L.C.; et al. Mitochondrial cristae shape determines respiratory chain supercomplexes assembly and respiratory efficiency. *Cell* **2013**, *155*, 160–171. [[CrossRef](#)] [[PubMed](#)]
3. Del Dotto, V.; Mishra, P.; Vidoni, S.; Fogazza, M.; Maresca, A.; Caporali, L.; McCaffery, J.M.; Cappelletti, M.; Baruffini, E.; Lenaers, G.; et al. OPA1 Isoforms in the Hierarchical Organization of Mitochondrial Functions. *Cell Rep.* **2017**, *19*, 2557–2571. [[CrossRef](#)] [[PubMed](#)]
4. Frezza, C.; Cipolat, S.; Martins de Brito, O.; Micaroni, M.; Beznoussenko, G.V.; Rudka, T.; Bartoli, D.; Polishuck, R.S.; Dhanraj, N.N.; De Strooper, B.; et al. OPA1 controls apoptotic cristae remodeling independently from mitochondrial fusion. *Cell* **2006**, *126*, 177–189. [[CrossRef](#)]
5. Ge, Y.; Shi, X.; Boopathy, S.; McDonald, J.; Smith, A.W.; Chao, L.H. Two forms of Opa1 cooperate to complete fusion of the mitochondrial inner-membrane. *eLife* **2020**, *9*, e50973. [[CrossRef](#)]
6. Rainbolt, T.K.; Saunders, J.M.; Wiseman, R.L. YME1L degradation reduces mitochondrial proteolytic capacity during oxidative stress. *EMBO Rep.* **2015**, *16*, 97–106. [[CrossRef](#)]
7. Wang, R.; Mishra, P.; Garbis, S.D.; Moradian, A.; Sweredoski, M.J.; Chan, D.C. Identification of new OPA1 cleavage site reveals that short isoforms regulate mitochondrial fusion. *Mol. Biol. Cell* **2021**, *32*, 157–168. [[CrossRef](#)]
8. Merkwirth, C.; Dargazanli, S.; Tatsuta, T.; Geimer, S.; Lower, B.; Wunderlich, F.T.; von Kleist-Retzow, J.C.; Waisman, A.; Westermann, B.; Langer, T. Prohibitins control cell proliferation and apoptosis by regulating OPA1-dependent cristae morphogenesis in mitochondria. *Genes. Dev.* **2008**, *22*, 476–488. [[CrossRef](#)]
9. Lee, H.; Smith, S.B.; Yoon, Y. The short variant of the mitochondrial dynamin OPA1 maintains mitochondrial energetics and cristae structure. *J. Biol. Chem.* **2017**, *292*, 7115–7130. [[CrossRef](#)]

10. Wai, T.; Garcia-Prieto, J.; Baker, M.J.; Merkwirth, C.; Benit, P.; Rustin, P.; Ruperez, F.J.; Barbas, C.; Ibanez, B.; Langer, T. Imbalanced OPA1 processing and mitochondrial fragmentation cause heart failure in mice. *Science* **2015**, *350*, aad0116. [[CrossRef](#)]
11. Wai, T.; Langer, T. Mitochondrial Dynamics and Metabolic Regulation. *Trends Endocrinol. Metab.* **2016**, *27*, 105–117. [[CrossRef](#)]
12. MacVicar, T.; Langer, T. OPA1 processing in cell death and disease—The long and short of it. *J. Cell Sci.* **2016**, *129*, 2297–2306. [[CrossRef](#)]
13. Noone, J.; O’Gorman, D.J.; Kenny, H.C. OPA1 regulation of mitochondrial dynamics in skeletal and cardiac muscle. *Trends Endocrinol. Metab.* **2022**, *33*, 710–721. [[CrossRef](#)]
14. Lee, H.; Smith, S.B.; Sheu, S.S.; Yoon, Y. The short variant of optic atrophy 1 (OPA1) improves cell survival under oxidative stress. *J. Biol. Chem.* **2020**, *295*, 6543–6560. [[CrossRef](#)]
15. Jang, S.; Javadov, S. OPA1 regulates respiratory supercomplexes assembly: The role of mitochondrial swelling. *Mitochondrion* **2020**, *51*, 30–39. [[CrossRef](#)]
16. Zamberlan, M.; Boeckx, A.; Muller, F.; Vinelli, F.; Ek, O.; Vianello, C.; Coart, E.; Shibata, K.; Christian, A.; Grespi, F.; et al. Inhibition of the mitochondrial protein Opa1 curtails breast cancer growth. *J. Exp. Clin. Cancer Res.* **2022**, *41*, 95. [[CrossRef](#)]
17. Tang, J.; Liu, Z.; Han, J.; Xue, J.; Liu, L.; Lin, J.; Wu, C.; Zhang, Q.; Wu, S.; Liu, C.; et al. Increased Mobile Zinc Regulates Retinal Ganglion Cell Survival via Activating Mitochondrial OMA1 and Integrated Stress Response. *Antioxidants* **2022**, *11*, 2001. [[CrossRef](#)]
18. Chapa-Dubocq, X.R.; Rodriguez-Graciani, K.M.; Guzman-Hernandez, R.A.; Jang, S.; Brookes, P.S.; Javadov, S. Cardiac Function is not Susceptible to Moderate Disassembly of Mitochondrial Respiratory Supercomplexes. *Int. J. Mol. Sci.* **2020**, *21*, 1555. [[CrossRef](#)]
19. Chapa-Dubocq, X.; Makarov, V.; Javadov, S. Simple kinetic model of mitochondrial swelling in cardiac cells. *J. Cell Physiol.* **2018**, *233*, 5310–5321. [[CrossRef](#)]
20. Jang, S.; Chapa-Dubocq, X.R.; Fossati, S.; Javadov, S. Analysis of Mitochondrial Calcium Retention Capacity in Cultured Cells: Permeabilized Cells Versus Isolated Mitochondria. *Front. Physiol.* **2021**, *12*, 773839. [[CrossRef](#)]
21. Scaduto, R.C., Jr.; Grotyohann, L.W. Measurement of mitochondrial membrane potential using fluorescent rhodamine derivatives. *Biophys. J.* **1999**, *76*, 469–477. [[CrossRef](#)] [[PubMed](#)]
22. Ban, T.; Heymann, J.A.; Song, Z.; Hinshaw, J.E.; Chan, D.C. OPA1 disease alleles causing dominant optic atrophy have defects in cardiolipin-stimulated GTP hydrolysis and membrane tubulation. *Hum. Mol. Genet.* **2010**, *19*, 2113–2122. [[CrossRef](#)] [[PubMed](#)]
23. Baek, M.L.; Lee, J.; Pendleton, K.E.; Berner, M.J.; Goff, E.B.; Tan, L.; Martinez, S.A.; Mahmud, I.; Wang, T.; Meyer, M.D.; et al. Mitochondrial structure and function adaptation in residual triple negative breast cancer cells surviving chemotherapy treatment. *Oncogene* **2023**, *42*, 1117–1131. [[CrossRef](#)] [[PubMed](#)]
24. Mendivil-Perez, M.; Velez-Pardo, C.; Jimenez-Del-Rio, M. TPEN induces apoptosis independently of zinc chelator activity in a model of acute lymphoblastic leukemia and ex vivo acute leukemia cells through oxidative stress and mitochondria caspase-3 and AIF-dependent pathways. *Oxid. Med. Cell Longev.* **2012**, *2012*, 313275. [[CrossRef](#)]
25. Garlid, K.D.; Paucek, P. The mitochondrial potassium cycle. *IUBMB Life* **2001**, *52*, 153–158. [[CrossRef](#)]
26. Rodriguez-Graciani, K.M.; Chapa-Dubocq, X.R.; MacMillan-Crow, L.A.; Javadov, S. Association between L-OPA1 Cleavage and Cardiac Dysfunction During Ischemia-Reperfusion Injury in Rats. *Cell Physiol. Biochem.* **2020**, *54*, 1101–1114. [[CrossRef](#)]
27. Li, H.; Qin, S.; Liang, Q.; Xi, Y.; Bo, W.; Cai, M.; Tian, Z. Exercise Training Enhances Myocardial Mitophagy and Improves Cardiac Function via Irisin/FNDC5-PINK1/Parkin Pathway in MI Mice. *Biomedicines* **2021**, *9*, 701. [[CrossRef](#)]
28. Boissan, M.; Montagnac, G.; Shen, Q.; Griparic, L.; Guitton, J.; Romao, M.; Sauvonnet, N.; Lagache, T.; Lasco, I.; Raposo, G.; et al. Membrane trafficking. Nucleoside diphosphate kinases fuel dynamin superfamily proteins with GTP for membrane remodeling. *Science* **2014**, *344*, 1510–1515. [[CrossRef](#)]
29. Chapa-Dubocq, X.R.; Garcia-Baez, J.F.; Bazil, J.N.; Javadov, S. Crosstalk between adenine nucleotide transporter and mitochondrial swelling: Experimental and computational approaches. *Cell Biol. Toxicol.* **2022**, *39*, 435–450. [[CrossRef](#)]
30. Rahn, J.J.; Stackley, K.D.; Chan, S.S. Opa1 is required for proper mitochondrial metabolism in early development. *PLoS ONE* **2013**, *8*, e59218. [[CrossRef](#)]
31. Hu, C.; Shu, L.; Huang, X.; Yu, J.; Li, L.; Gong, L.; Yang, M.; Wu, Z.; Gao, Z.; Zhao, Y.; et al. OPA1 and MICOS Regulate mitochondrial crista dynamics and formation. *Cell Death Dis.* **2020**, *11*, 940. [[CrossRef](#)]
32. Patten, D.A.; Wong, J.; Khacho, M.; Soubannier, V.; Mailloux, R.J.; Pilon-Larose, K.; MacLaurin, J.G.; Park, D.S.; McBride, H.M.; Trinkle-Mulcahy, L.; et al. OPA1-dependent cristae modulation is essential for cellular adaptation to metabolic demand. *EMBO J.* **2014**, *33*, 2676–2691. [[CrossRef](#)]
33. Griparic, L.; Kanazawa, T.; van der Blik, A.M. Regulation of the mitochondrial dynamin-like protein Opa1 by proteolytic cleavage. *J. Cell Biol.* **2007**, *178*, 757–764. [[CrossRef](#)]
34. Anand, R.; Wai, T.; Baker, M.J.; Kladt, N.; Schauss, A.C.; Rugarli, E.; Langer, T. The i-AAA protease YME1L and OMA1 cleave OPA1 to balance mitochondrial fusion and fission. *J. Cell Biol.* **2014**, *204*, 919–929. [[CrossRef](#)]
35. Sprenger, H.G.; Wani, G.; Hesseling, A.; Konig, T.; Patron, M.; MacVicar, T.; Ahola, S.; Wai, T.; Barth, E.; Rugarli, E.I.; et al. Loss of the mitochondrial i-AAA protease YME1L leads to ocular dysfunction and spinal axonopathy. *EMBO Mol. Med.* **2019**, *11*, e9288. [[CrossRef](#)]
36. Quiros, P.M.; Ramsay, A.J.; Sala, D.; Fernandez-Vizarra, E.; Rodriguez, F.; Peinado, J.R.; Fernandez-Garcia, M.S.; Vega, J.A.; Enriquez, J.A.; Zorzano, A.; et al. Loss of mitochondrial protease OMA1 alters processing of the GTPase OPA1 and causes obesity and defective thermogenesis in mice. *EMBO J.* **2012**, *31*, 2117–2133. [[CrossRef](#)]

37. Larrue, C.; Mouche, S.; Lin, S.; Simonetta, F.; Scheidegger, N.K.; Poulain, L.; Birsén, R.; Sarry, J.E.; Stegmaier, K.; Tamburini, J. Mitochondrial fusion is a therapeutic vulnerability of acute myeloid leukemia. *Leukemia* **2023**, *37*, 765–775. [[CrossRef](#)]
38. Tobacyk, J.; Parajuli, N.; Shrum, S.; Crow, J.P.; MacMillan-Crow, L.A. The first direct activity assay for the mitochondrial protease OMA1. *Mitochondrion* **2019**, *46*, 1–5. [[CrossRef](#)]
39. Garcia-Perez, C.; Roy, S.S.; Naghdi, S.; Lin, X.; Davies, E.; Hajnoczky, G. Bid-induced mitochondrial membrane permeabilization waves propagated by local reactive oxygen species (ROS) signaling. *Proc. Natl. Acad. Sci. USA* **2012**, *109*, 4497–4502. [[CrossRef](#)]
40. Mishra, P.; Varuzhanyan, G.; Pham, A.H.; Chan, D.C. Mitochondrial Dynamics is a Distinguishing Feature of Skeletal Muscle Fiber Types and Regulates Organellar Compartmentalization. *Cell Metab.* **2015**, *22*, 1033–1044. [[CrossRef](#)]
41. Gomes, L.C.; Di Benedetto, G.; Scorrano, L. During autophagy mitochondria elongate, are spared from degradation and sustain cell viability. *Nat. Cell Biol.* **2011**, *13*, 589–598. [[CrossRef](#)] [[PubMed](#)]
42. Labbe, K.; Murley, A.; Nunnari, J. Determinants and functions of mitochondrial behavior. *Annu. Rev. Cell Dev. Biol.* **2014**, *30*, 357–391. [[CrossRef](#)] [[PubMed](#)]
43. Liesa, M.; Shirihai, O.S. Mitochondrial dynamics in the regulation of nutrient utilization and energy expenditure. *Cell Metab.* **2013**, *17*, 491–506. [[CrossRef](#)] [[PubMed](#)]
44. Benard, G.; Bellance, N.; James, D.; Parrone, P.; Fernandez, H.; Letellier, T.; Rossignol, R. Mitochondrial bioenergetics and structural network organization. *J. Cell Sci.* **2007**, *120*, 838–848. [[CrossRef](#)]
45. Kuznetsov, A.V.; Javadov, S.; Margreiter, R.; Grimm, M.; Hagenbuchner, J.; Ausserlechner, M.J. Structural and functional remodeling of mitochondria as an adaptive response to energy deprivation. *Biochim. Biophys. Acta Bioenerg.* **2021**, *1862*, 148393. [[CrossRef](#)]
46. Loor, G.; Schumacker, P.T. Role of hypoxia-inducible factor in cell survival during myocardial ischemia-reperfusion. *Cell Death Differ.* **2008**, *15*, 686–690. [[CrossRef](#)]
47. Javadov, S.; Rajapurohitam, V.; Kilic, A.; Hunter, J.C.; Zeidan, A.; Said Faruq, N.; Escobales, N.; Karmazyn, M. Expression of mitochondrial fusion-fission proteins during post-infarction remodeling: The effect of NHE-1 inhibition. *Basic. Res. Cardiol.* **2011**, *106*, 99–109. [[CrossRef](#)]
48. Ban, T.; Kohno, H.; Ishihara, T.; Ishihara, N. Relationship between OPA1 and cardiolipin in mitochondrial inner-membrane fusion. *Biochim. Biophys. Acta Bioenerg.* **2018**, *1859*, 951–957. [[CrossRef](#)]
49. Roy, M.; Reddy, P.H.; Iijima, M.; Sesaki, H. Mitochondrial division and fusion in metabolism. *Curr. Opin. Cell Biol.* **2015**, *33*, 111–118. [[CrossRef](#)]
50. Westermann, B. Bioenergetic role of mitochondrial fusion and fission. *Biochim. Biophys. Acta* **2012**, *1817*, 1833–1838. [[CrossRef](#)]
51. Mishra, P.; Carelli, V.; Manfredi, G.; Chan, D.C. Proteolytic cleavage of Opa1 stimulates mitochondrial inner membrane fusion and couples fusion to oxidative phosphorylation. *Cell Metab.* **2014**, *19*, 630–641. [[CrossRef](#)]

Disclaimer/Publisher’s Note: The statements, opinions and data contained in all publications are solely those of the individual author(s) and contributor(s) and not of MDPI and/or the editor(s). MDPI and/or the editor(s) disclaim responsibility for any injury to people or property resulting from any ideas, methods, instructions or products referred to in the content.